Proceedings of the
44th IEEE Conference on Decision and Control, and
the European Control Conference 2005
Seville, Spain, December 12-15, 2005

An Adaptive Predictive Approach to Emergency Frequency Control in Electric Power Systems

Mats Larsson

Abstract— **Wide-area phasor measurements and modern communication techniques will provide access to system-wide frequency data with high accuracy and small time delay. This will make it possible also to monitor and control also relatively fast phenomena such as frequency instability using centralized approaches. This paper describes the decision logic of a centralized emergency frequency controller based on predictive control. A single machine equivalent for each power system island is computed online using phasor measurements. Using this model the progression of frequency stability after a contingency is monitored and stabilizing load shedding is determined in a coordinated way for the supervised area of the power system.**

I. Introduction

Electric power systems are designed, through careful planning and preventive control schemes, to survive most foreseeable disturbances [1]. Not all possible disturbances, however, can be foreseen at the planning stage and these may result in instability that will eventually lead to collapse or islanding of the system. The objective of an emergency control system is to detect such situations and carry out control actions necessary to prevent collapse of the system. Increasing demand on the power system increases the likelihood of system problems such as instabilities and collapses. While it is not possible to predict or prevent all contingencies that may lead to power system collapse, a wide area protection system that provides a reliable security prediction and optimized coordinated actions is able to mitigate or prevent large area disturbances.

The main tasks are early recognition of instabilities and stabilizing the power system by corrective actions when necessary. With a system wide protection scheme, operators can increase power system availability and more accurately coordinate load shedding and other corrective control actions than they can with traditional local schemes.

Frequency stability, which is studied in this paper, denotes the ability of a power system to operate with the (average) system frequency within normal operating limits. Failure to do so may cause damage to generation and/or load side equipment, and power plants are most often equipped with underfrequency protection relays that disconnect the plant if the network frequency is lower than say 47 Hz for a 50 Hz system or 56-57 Hz for a 60 Hz system. Disconnection of a first plant due to underfrequency protection often becomes catastrophic, since the tripping of the first plant further accelerates frequency decline and usually triggers a cascade of plant trippings and subsequently a system-wide blackout.

M. Larsson is with Corporate Research, ABB Switzerland, 5405 Baden, Switzerland. (mats.larsson@ch.abb.com)

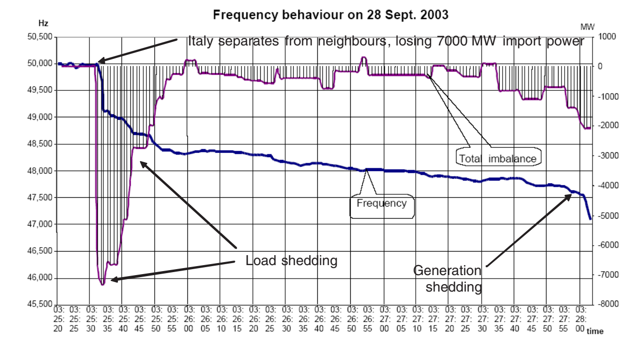

Fig. 1. The frequency and estimated power imbalance during the Italian grid collapse of 2003 [3].

Underfrequency load shedding (UFLS) is the most widely used protection against frequency instability. Such a scheme is based on many individual relays spread out of the power system. Each relay can typically shed load in several steps of 5–20 % (of the total feeder load) each when a local frequency measurement becomes lower than a threshold value. Typical threshold values are 57–58.5 Hz for 60 Hz systems or 48–48.5 Hz for a 50 Hz system [2]. Usually there is also a time-delay intended for noise rejection. The aim of such a scheme is to disconnect enough load to stabilize the frequency before the plant underfrequency relays operate.

The main drawback of these schemes is their delayed response since they must wait for the frequency to decline before taking action. Tuning of the local scheme, which involves selecting multiple frequency settings for each relay, is usually done using off-line simulation studies. Tuning therefore requires much engineering work and it can not be guaranteed that the scheme works well also in operating conditions other than those assumed in the off-line tuning study.

It is well known (see e.g., [4]) that the power imbalance (ΔP) following the outage of a generator or a tie-line can be calculated from the initial rate-of-change of the frequency and the system inertia constant according to the formula

$$\Delta P = 2\frac{\mathrm{d}\omega}{\mathrm{d}t} H_{system} \quad (1)$$

This value can be used as an indication of the amount of load that has to be shed to arrest further frequency decline. The method described in this paper works by accurately monitoring these two quantities using quantities from a wide-area measurement system.

An illustration of the relation between the power imbalance and frequency decline can be seen in can be seen in Fig. 1 where the frequency and estimated power imbalance in Italy during the 2003 blackout is shown [3]. Initially following the grid separation at 03:25:30, there is a 7000 MW negative power imbalance in Italy, and a sharp decline of the frequency down to about 49.2 Hz can be observed. Load shedding actions are taken by local relays and this greatly reduces the power imbalance. However the shedding carried out is not enough and the frequency continues to slowly decay and eventually the critical frequency of 47.6 Hz is reached. Then underfrequency protection starts to trip generation and a rapid frequency collapse starts, which leads to a blackout about two and a half minutes after the initial disturbance at around 03:28:00.

The post-analysis of the Italy event described above and also other similar events in other countries shows that the conventional protection approach with local frequency relays is not always adequate.

This paper demonstrates an adaptive predictive method that aims to overcome some of the limitations of the conventional local approach. The adaptive aspects of the scheme aims to extract the relevant power system parameters from on-line measurements, and base the control based on that rather than a fixed pre-programmed response determined in an off-line tuning study. Therefore the scheme can adapt its sensitivity to the current operating conditions, eliminating the need for many assumptions that have to made when tuning the conventional local scheme. In this adaptive step relevant system parameters are extracted from the wide-area measurements and a reduced single-machine equivalent is constructed. In the predictive step, this model is used to estimate an expected steady-state frequency following a disturbance using a model-predictive approach. Based on this prediction it can be determined whether or not emergency control actions are necessary. In that case, a search method is applied to explore the various available options and select the optimal one.

II. System Setup

The wide area platform for dynamic monitoring of transmission systems comprises of hardware:

- Phasor Measurement Units (PMU)
- Communication Links
- Central Unit (Personal Computer)

and software:

- Data preprocessing package
- Basic services
- Specific individual applications
- Graphical user interface (GUI)
- Package containing model/data of the supervised power system and coordination with other software packages

PMUs are placed in the substations to allow observation of a critical part of the supervised power system under any operation conditions (network islanding, outages of lines, generators etc.), taking into account a certain degree of redundancy to provide sufficient results also in a case of unavailability of some data (PMU outage, communication failure etc.). Measured data are sent via dedicated communication channels/links to a central unit, which is a central computational unit where the collected measurements are synchronized and sorted, yielding the snapshot of the power system state. This setup is shown in Fig. 2. The snapshot is then processed by the Basic Services package (BS), which is part of the central unit. Basic Services denote the set of algorithms included in all installations of the wide area platform for different applications and they are comprising the following capabilities:

- ability to provide needed data for any application
- fast execution - leaving sufficient time for running applications within the sampling interval
- robustness - resistance against poor quality of some input data (unavailability, out of range, synchronization problems etc.)

Applications, which are attached to the output of BS, address various phenomena occurring in power systems, such as frequency instability, voltage instability etc. They predict the state of the power system and trigger appropriate actions if an incipient instability is detected. The controller described in the paper is one example of such an application. Their output as well as the output of BS are displayed to the power system operator by an ergonomic GUI. The functional structure described above is illustrated in Fig. 3.

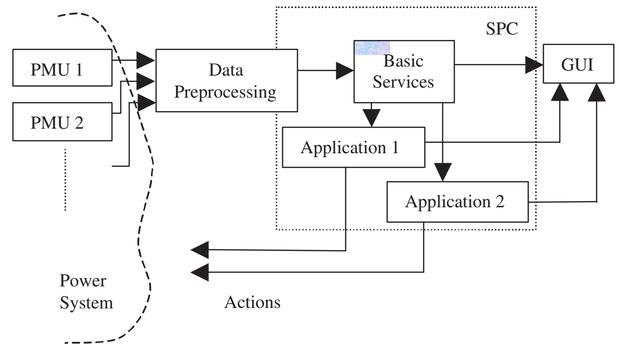

Fig. 3. Functional architecture of wide area measurement platform based on synchronized phasor measurements.

III. The Test System

In order to illustrate the method, simulations are carried out using the simple two-area test system shown in Fig. 4. It is based on data given in reference [5]. Each load is assumed to consist of five identical feeders that can be switched out independently when there is a need for load shedding. The generators are modelled using standard 6th order models with first order fast excitation systems and constant power governors.

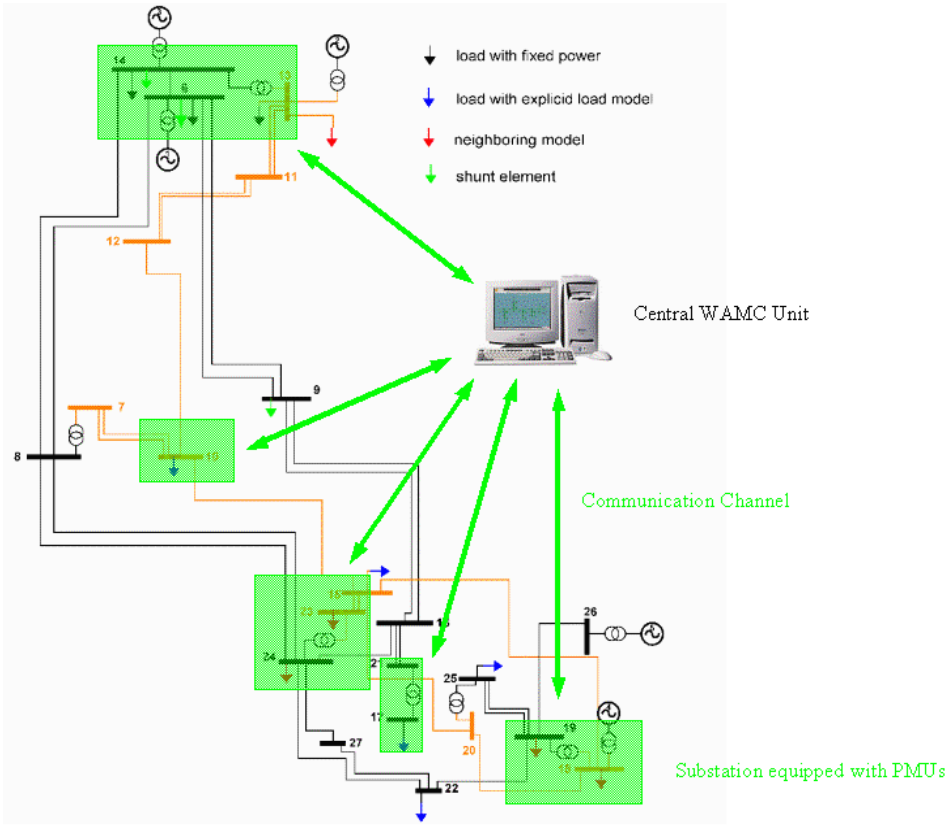

Fig. 2. Setup of wide area platform based on synchronized phasor measurements.

To simulate the effect of measurement noise, random 0.01 Hz additive errors have been introduced on the generator speed measurements and 0.02 % multiplicative errors on the amplitudes and phase angles of the voltage and current phasors. These assumptions correspond to about twice the noise levels specified by manufacturers of PMUs. Communication delays of 0.25 s in either direction between the PMUs and the central processing unit and a computational delay of 0.25 s have also been included in the employed simulation model.

IV. Adaptive Model Predictive Control Strategy

The execution of the proposed method consists of separate steps as follows. First, a single-machine equivalent model of the system is formed based on the collected measurements. In the next step, the model is employed continuously used to estimate the active power imbalance in the system. Using the this estimation and the single-machine equivalent model, an expected steady-state frequency can be predicted whenever a frequency excursion is detected. Should this predicted steady-state frequency be unacceptable, the amount of load shedding required to keep the frequency above some target value is calculated. In the final step, the calculated amount is allocated to different feeders using a simple iterative method considering the actual load on the feeders.

A. On-line Model Adaptation

The method is based on a single generator model of each power system island as proposed by [4]. The parameters in this model is being continuously adapted at every time step the algorithm operates.

However, the conservative assumption that the effect of governors can be neglected is made. The frequency dynamics can then be described by the differential equation

$$\frac{\mathrm{d}\omega}{\mathrm{d}t} = \frac{1}{2H_{system}}(P_m - P_e) \tag{2}$$

where H_i is the inertia constant of generator i and H_{system} is the system inertia constant defined as follows

$$H_{system} = \sum_{1..N} H_i \tag{3}$$

$$P_m = \sum_{1..N} P_{m,i} \tag{4}$$

$$P_e = P_{loss} + \sum_{1..M} P_{l,i} \tag{5}$$

The constants N and M is the number of generators and loads, respectively. The active power losses are denoted P_{loss}, the load consumed at bus i is denoted $P_{l,i}$, the mechanical power delivered to the shaft of generator i is denoted $P_{m,i}$, and the system average frequency is denoted ω.

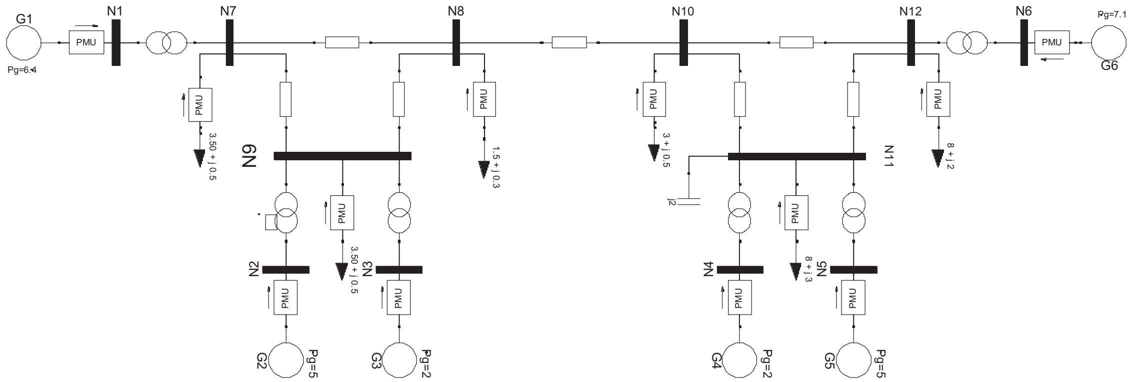

Fig. 4. The employed test system.

Each load is modelled using a static load model

$$P_{l,i} = (1-k_i)P_{0,i}(\frac{V_i}{V_{0,i}})^{a_{s,i}}(1+c_i(\omega-\omega_s)) \quad (6)$$

$$Q_{l,i} = (1-k_i)Q_{0,i}(\frac{V_i}{V_{0,i}})^{b_{s,i}}(1+d_i(\omega-\omega_s)) \quad (7)$$

where k_i is an input signal modelling load shedding for each load, $V_{0,i}$ is the nominal voltage, $P_{0,i}$ the nominal load and ω_s is the synchronous frequency. The parameters a_i, b_i, c_i and d_i in the load model (8)–(9) can be determined from measurements taken at (at least) three different samples. The parameter identification triggers when the system average frequency deviation is becomes greater than 0.2 Hz or a frequency derivative greater than 0.3 Hz/s. Measurement samples are then collected until a sufficiently large frequency variation has occurred, and the load parameters are then estimated in a least-squares manner according to [6].

Linearizing the load model and writing on vectorized form yields

$$\Delta P_L = A\Delta V + C\Delta\omega + G\Delta k \quad (8)$$

$$\Delta Q_L = B\Delta V + D\Delta\omega + H\Delta k \quad (9)$$

where $A = \mathbf{diag}(a_1 \dots a_M)$, $B = \mathbf{diag}(b_1 \dots b_M)$ etc.

To account for the effect of voltage variations on the load, the model proposed by [4] is augmented with matrices of sensitivity coefficients

$$\Delta V = E\Delta P_L \quad (10)$$

$$\Delta V = F\Delta Q_L \quad (11)$$

After combining (2) and (8)-(11) to eliminate the variables ΔV, ΔP_L and ΔQ_L, the model can be written on the ordinary differential equation form

$$\frac{\mathrm{d}\Delta x}{\mathrm{d}t} = A_{ode}\Delta x + B_{ode}\Delta k + E_{ode}\Delta d \quad (12)$$

$$\Delta y = C_{ode}\Delta x \quad (13)$$

where x is the dynamical state vector. In the application in this paper, the state vector contains only the system average frequency and is thus a scalar. Also other dynamic states can be included, such as the states of an equivalent governor model or dynamic load models. Δk is a vector of the load shedding inputs and Δd is a disturbance input, modelling for example generator trippings. Note that all equations are now written on incremental form, that is, relative to the current operating point. $\Delta x = x - x_0$, $\Delta y = y - y_0$ and $\Delta k = k - k_0$ where x_0, y_0 and k_0 are the values of the respective variables at the linearization point. In postcontingency cases it is not unlikely that the network has been split into two or more separate islands. In those cases, a single machine equivalent according to (12)-(13) is formed for each island.

B. Frequency Stability Monitoring–Timing of Shedding

Using the continuously adapted single-machine equivalent (12)-(13), a steady state frequency can be calculated. Furthermore, the current power mismatch can be estimated as

$$\Delta d = 2H_{system}\,\dot{\omega}_{avg\_filt}(k) \quad (14)$$

The island average frequency is supplied by the wide-area measurement system which forms this by averaging frequency measurements from as many PMUs as possible, and the system inertia can either be estimated during the initial phase of the disturbance together with the load parameter or supplied as a parameter by the wide-area measurement system.

Using the power mismatch as estimated by (14), the predicted steady-state frequency can be estimated as

$$\Delta y^* = -C_{ode}A_{ode}^{-1}(B_{ode}\Delta k + E_{ode}\Delta d) \quad (15)$$

At this stage, it is assumed that no load shedding control is made, i.e, $\Delta k = 0$, so the predicted steady-state frequency is written

$$\Delta y^* = -C_{ode}A_{ode}^{-1}E_{ode}\Delta d \quad (16)$$

Subsequently, the predicted actual frequency is found using

$$y^* = \Delta y^* + y_0 \quad (17)$$

Fig. 5 illustrates the accuracy of the estimated minimum frequency without load shedding for a case with sequential tripping of generators G3 at 10.1 s, G4 at 85.2 s and G5 at 160 s. This corresponds to one third of the pre-disturbance generation. Note that the last tripping is an unrealistically large disturbance that is used only to illustrate that there is some inexactness in the method due to the assumption that the network is linear. For the two previous trippings, the method accurately predicts the final frequency in 1-2 seconds.

Fig. 6 shows the steady-state frequency prediction error in the same scenario. We can see a sharp increase in the prediction error for the first few samples after each trip. This is due to a one sample time delay before the plant trips are noticed and subsequently to the time it takes for the frequency derivative estimate to converge. Following this initial spike, there is then a slower transient due to the errors introduced by the linearization of the network equations. As the frequency approaches its steady-state value this error component also converges to zero.

C. Calculation of Required Amount of Shedding

Assume that a certain steady-state frequency $y^* = \Delta y^* + y_0$ has been calculated using (16) and that this predicted frequency is found to be unacceptable. The required amount of load to shed can be found by setting $B_{ode} = 1/(2H_{system})$, thus assuming that all load is shed in a single point. The power step that needs to be applied to keep the steady-state frequency estimate at a certain target value y^*_{ref} can then be determined from (15) where

$$\Delta P = -\frac{(y^*_{ref} - y_0) + C_{ode}A^{-1}_{ode}E_{ode}\Delta d}{C_{ode}A^{-1}_{ode}B_{ode}} \tag{18}$$

Fig. 7 shows the frequency response following disconnection of the two units G3 and G4. At time 60 s, (18) suggests that 1.16 p.u. of active load needs to be shed to restore the frequency to a target value of 49 Hz. Following shedding, the frequency reaches a new steady-state at about 48.95 Hz. To illustrate the accuracy of the prediction also for cases where the system frequency dynamics have not yet settled, a second trip is applied at 86.5 s. At time 90 s, an amount of 2.15 p.u. is shed, and the frequency reaches a new steady-state at about 48.8 Hz.

On both occasions, the shedding is emulated by a fictitious generation unit (PQ-node) at bus 8 which injects the required amount of active power. As shown in the figure, the calculated amount is reasonably accurate on both occasions.

D. Choice of Shedding Locations

The last step is to assign the calculated amount of shedding to the feeders where load is available for shedding. The very basic, yet efficient, algorithm we employ in this paper is:

1) Calculate the amount of load required for shedding using (18).
2) Find loads with available steps, and calculate their actual step size, that is, taking the actual load on the feeders into account.

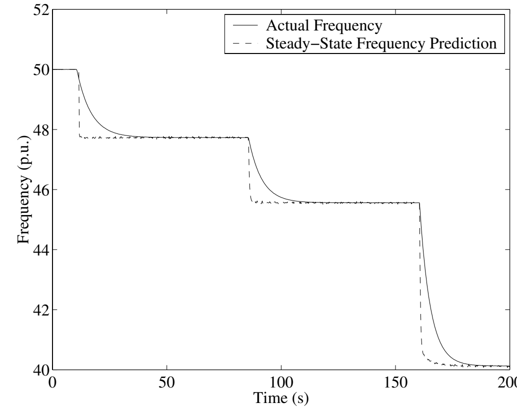

Fig. 5. Frequency response and steady-state frequency prediction in the simulation with disconnection of the three units G3, G4 and G5 at 10.1 s, 85.2 s and 160 s, respectively.

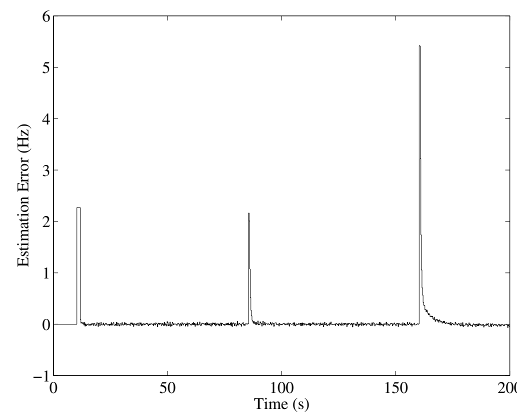

Fig. 6. Steady-state frequency frequency prediction error following the three unit trippings.

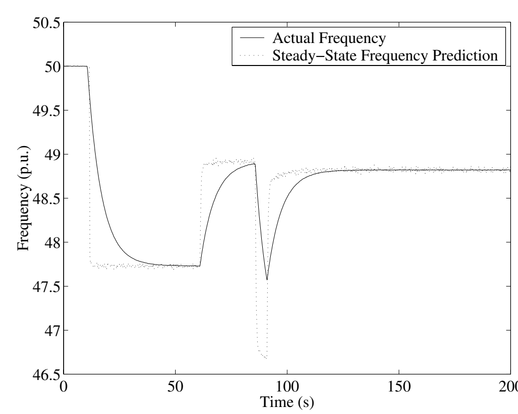

Fig. 7. Application of power steps calculated according to (18).

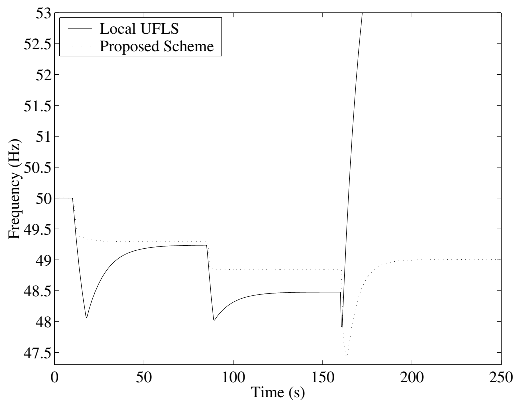

Fig. 8. Comparison of frequency response with local UFLS and the proposed scheme.

3) Allocate one step of load shedding at the load with the step size closest to the remaining amount to shed.
4) Repeat step 3 until at least the amount of load calculated in step 1 has been shed.

V. Closed Loop Operation

The simulations in the previous sections have been presented as illustrations of the various aspect of the proposed method, such as its inaccuracy and computational procedure. In this final section of simulation results we present closed loop simulation results to illustrate the method. For comparison we present simulation results with local underfrequency load shedding (UFLS) relays employing the same control step sizes at each load bus. The local relays have been tuned to shed 20 % of the load at the frequencies 48, 47.8, 47.6 Hz with a random time delays between 0.1-0.2 s.

Fig. 8 shows the frequency response following the disconnection of the three units, with local UFLS and the proposed scheme. We see that when the two small units are tripped at 10 and 86 s, respectively, the local UFLS scheme reacts later since is has to wait for the frequency to decline sufficiently before ordering corrective action. On the other hand, the proposed scheme applies stabilizing actions as soon as they can be accurately calculated and the frequency decline is therefore arrested earlier. Another observation that can be made is that the reaction time, and thereby the frequency decline, is slightly smaller at the second trip since no time is spent estimating the load parameters. When the large unit is tripped, the frequency decline is actually larger with the proposed scheme than with the local scheme because of the time-delays introduced by communication and centralized calculation. However, the local scheme uses an excessive amount of shedding and a considerable frequency overshoot is present.

VI. Future Work

In a real system, the load model (12)-(13) will not be an exact model of the load demand. The impact of various load types on the proposed method is a subject for further study. Also dynamic models could be used if the state vector in (12) is extended. The effect of governor controls could be included in a similar manner. Note however, that the parameters for these dynamic load and governor models may be difficult to to obtain since they require estimation over a prolonged time window. In this paper we use a heuristic method to select which loads to shed. Since the location of the shedding is not critical from a frequency stability point of view, the selection could be done based on other criteria, such as to minimize overvoltages or steady-state angle differences, or to consider prioritization or shedding rotation.

VII. Conclusion

An adaptive predictive approach to frequency stability control has been presented. A single-machine model of each power system island and its connected load and generation is formed based on wide-are phasor measurements. This model is used to monitor frequency stability and determine the correct amount of load or generation to shed in order to restore the frequency to a target value. Since control determination is based on a predictive strategy, the proposed method avoids the delayed response of traditional underfrequency load shedding relays.

References

[1] P. Kundur, *Power System Stability and Control*, ser. Power System Engineering Series. McGraw-Hill, New York, 1994.
[2] CIGRE, "System protection schemes in power networks," CIGRE Task Force 38.02.19, Tech. Rep., 2000.
[3] "Final report of the investigation committee on the 28 september 2003 blackout in italy," UCTE, Tech. Rep., April 2004.
[4] P. M. Anderson and M. Mirheydar, "A low-order system frequency response model)," *IEEE Transactions on Power Systems*, vol. 5, no. 4, pp. 720–9, August 1990.
[5] D. Prasetijo, W. R. Lachs, and D. Sutanto, "A new load shedding scheme for limiting underfrequency," *IEEE Transactions on Power System*, vol. 9, no. 3, pp. 1371–78, August 1994.
[6] R. Johansson, *System Modelling and Identification*. Prentice-Hall, 1993.